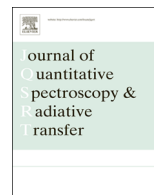




Contents lists available at SciVerse ScienceDirect

Journal of Quantitative Spectroscopy & Radiative Transfer

journal homepage: www.elsevier.com/locate/jqsrt

Intensity and polarization of dust aerosols over polarized anisotropic surfaces

K.N. Liou^a, Y. Takano^{a,*}, P. Yang^b^a Joint Institute for Earth System Science and Engineering, Department of Atmospheric and Oceanic Sciences, University of California, Los Angeles, CA 90095, USA^b Department of Atmospheric Sciences, Texas A&M University, College Station, TX 77845, USA

ARTICLE INFO

Article history:

Received 1 February 2013

Received in revised form

10 May 2013

Accepted 13 May 2013

Available online 21 May 2013

Keywords:

Surface albedo and polarization

Dust aerosols

Phase matrix elements

Degree of linear polarization

Bidirectional reflectance

Remote sensing

ABSTRACT

The effect of surface polarization on the intensity and linear polarization patterns of sunlight in an atmosphere containing a dust aerosol layer is investigated by means of the adding principle for vector radiative transfer in which the surface is treated as a layer without transmission. We present a number of computational results and analysis for three cases: Lambertian (unpolarized isotropic), polarized isotropic, and polarized anisotropic surfaces. An approach has been developed to reconstruct anisotropic 2×2 phase matrix elements on the basis of bidirectional-reflectance and linear-polarization patterns that have been measured from polarimeters over various land surfaces. The effect of surface polarization on the simulated intensity patterns over a dust layer is shown to be negligible. However, the differences in the simulated linear polarization patterns between commonly assumed Lambertian and polarized anisotropic cases are substantial for dust optical depths between 0.1 and 0.5 and for surface albedos of 0.07 and 0.4, particularly in backward directions.

© 2013 Elsevier Ltd. All rights reserved.

1. Introduction

Intensity and polarization of sunlight reflected from aerosols and clouds have been shown to bear a strong imprint of their size, shape, optical depth, and other optical properties. Perhaps the most intriguing results associated with the use of polarization data for inferring particle size and optical properties have been found in the study of Venus' cloud deck by the French astronomer Lyot [1]. In a subsequent work, Hansen and Hovenier [2] performed an extensive multiple scattering investigation and determined from the linear polarization data that the Venus cloud layer is composed of spherical particles (rainbow feature) having a mean radius of $\sim 1.05 \mu\text{m}$ and a real refractive index of ~ 1.44 at a wavelength of $0.55 \mu\text{m}$.

The NASA Glory mission (Mishchenko et al. [3]) had the similar idea of using the reflected spectral polarization of sunlight from the Earth's atmosphere without clouds to determine the optical and thermodynamic properties of aerosols, including absorbing black carbon and dust particles.

The NASA Glory spacecraft unfortunately failed to reach orbit after liftoff on March 4, 2011. An attempt, however, has been initiated to reengage the polarization instrument, referred to as Aerosol Polarimetric Sensor (APS), to collect polarimetric measurements along satellite ground track. In order to determine the physical and chemical properties as well as the spatial and temporal distributions of aerosols, APS will measure polarized reflected sunlight in the wavelength range of $0.4\text{--}2.4 \mu\text{m}$. Because aerosol optical depths are usually small ($\tau < \sim 1$), it appears that the effect of surface reflection cannot be neglected, especially over bright land surfaces. Furthermore, the effect of surface polarization properties with reference to the nature of

* Corresponding author. Tel.: +1 310 794 9832; fax: +1 310 794 9796.
E-mail address: ytakano@atmos.ucla.edu (Y. Takano).

anisotropy on polarization signals at the top of the atmosphere has not been carefully considered in radiative transfer simulations involving aerosols and thin cirrus clouds, although a number of recent studies have addressed the effect of surface polarization [4–6].

The objective of this paper is to explore the surface polarization effect on the simulated polarization patterns in an atmosphere containing dust particles. Specifically, we have extended the surface polarization model by taking into consideration recent observations of the polarized bidirectional reflectance from land surfaces. Moreover, the database for the single-scattering of dust aerosols developed by Meng et al. [7] has been used, along with the adding method for radiative transfer of polarized light to compute the reflected intensity and polarization patterns at the top of a dust layer to understand the significance of surface polarization.

This paper is organized as follows. First, we present the single-scattering properties of randomly oriented dust particles using a tri-axial ellipsoidal model in Section 2. This is followed by a discussion in Section 3 on the Stokes parameters and phase matrix in the content of vector radiative transfer using the adding/doubling approach and the definition of surface reflection matrix and its elements under various approximations. We have also presented a number of computational results and analysis for cases involving Lambertian (unpolarized isotropic), polarized isotropic, and polarized anisotropic surfaces. For the last case, an approach has been developed to reconstruct 2×2 phase matrix elements on the basis of the bidirectional-reflectance and linear-polarization patterns that have been measured over various land surfaces.

2. Optical properties of dust aerosols

Airborne mineral dust originates primarily in desert and semi-arid regions and is globally distributed. Accurate determination of its single-scattering properties is fundamental to quantifying aerosol radiative forcing and critical to developing appropriate remote sensing techniques for the detection of its size, shape, and composition. Electron microscopic images reveal that mineral dust particles are almost exclusively nonspherical and have irregular shapes with no specific habits. Due to technical difficulties, experimental determinations of the extinction efficiency, single-scattering albedo and scattering phase matrices around the forward and backward scattering directions have not been solely determined from measurements. Also, measurements are usually conducted at visible wavelengths with a small number of dust samples. The applicability of experimental approaches to the study of the single-scattering properties of dust particles throughout the entire solar and thermal infrared spectra cannot be carried out in practical terms.

Bi et al. [8] investigated the single-scattering properties of a tri-axial ellipsoidal model by introducing an additional degree of morphological freedom to reduce the symmetry of spheroids. They demonstrated that the optical properties computed from the ellipsoidal model with optimally selected particle shapes and their weightings more closely matched laboratory measurements. Additionally, the results

computed from the ellipsoidal model fit measurements better than the spheroidal model, particularly in the case of the phase matrix elements associated with polarization. Meng et al. [7] developed a database for the single-scattering properties and phase matrix elements for dust particles assuming tri-axial ellipsoids based on the computational results from a combination of the T -matrix method [9], the discrete dipole approximation [10], and an improved geometric optics method [11,12]. The database covers various aspect ratios and size parameters ranging from Rayleigh to geometric optics regimes.

In the following, we discuss the scattering phase matrix for dust aerosols. If no assumption is made about particle orientation, the “scattering phase matrix” for a set of nonspherical particles contains 16 elements, P_{ij} ($i, j=1-4$), and can be expressed as follows:

$$\mathbf{P} = \begin{bmatrix} P_{11} & P_{12} & P_{13} & P_{14} \\ P_{21} & P_{22} & P_{23} & P_{24} \\ P_{31} & P_{32} & P_{33} & P_{34} \\ P_{41} & P_{42} & P_{43} & P_{44} \end{bmatrix}. \quad (1)$$

However, if nonspherical particles are assumed to be randomly oriented in space and their mirror images have equal numbers such that the reciprocity principle can be applied for incoming and outgoing light beams, the scattering phase matrix can be reduced to six independent elements in the form [13,14]

$$\mathbf{P}(\theta) = \begin{bmatrix} P_{11} & P_{12} & 0 & 0 \\ P_{12} & P_{22} & 0 & 0 \\ 0 & 0 & P_{33} & -P_{43} \\ 0 & 0 & P_{43} & P_{44} \end{bmatrix}. \quad (2)$$

In this case, the six elements are a function of the scattering angle θ , defined by the directions of the incoming and outgoing light beams.

In order to use the database presented in [7] for dust particles assumed ellipsoid in shape, we must specify three semi-axis lengths (a , b , and c) to define the shape, where a and b are two semi-minor and semi-major axes of the equatorial ellipse, and c is the polar radius. For a given complex refractive index m for dust, its single-scattering properties are interpolated from the database for computational purposes. Also, the database includes the kernel look-up tables $K_{sca/ext/abs}$ and K_{ij} for dust size distributions, where the notations sca , ext , and abs denote the scattering, extinction, and absorption, respectively, and ij denotes scattering phase matrix elements. For a given size distribution $dN_x/d\ln x$, the averaged scattering properties are given by

$$\bar{c}_{sca} \bar{P}_{ij}(\theta) = \sum_m \frac{dN_x(x^m)}{d\ln x} K_{ij}(\theta, x^m), \quad (3a)$$

$$\bar{c}_{sca/ext/abs} = \sum_m \frac{dN_x(x^m)}{d\ln x} K_{sca/ext/abs}, \quad (3b)$$

where x^m is the center of the m th bin and the size parameter x is defined by $2\pi r/\lambda$, where λ is the wavelength of incident light.

Download English Version:

<https://daneshyari.com/en/article/5428787>

Download Persian Version:

<https://daneshyari.com/article/5428787>

[Daneshyari.com](https://daneshyari.com)